World Academy of Science, Engineering and Technology
International Journal of Electrical and Computer Engineering
Vol:11, No:6, 2017

Estimation of the Temperatures in an Asynchronous Machine Using Extended Kalman Filter

Yi Huang, Clemens Guehmann

***Abstract*—**In order to monitor the thermal behavior of an asynchronous machine with squirrel cage rotor, a 9th-order extended Kalman filter (EKF) algorithm is implemented to estimate the temperatures of the stator windings, the rotor cage and the stator core. The state-space equations of EKF are established based on the electrical, mechanical and the simplified thermal models of an asynchronous machine. The asynchronous machine with simplified thermal model in *Dymola* is compiled as *DymolaBlock*, a physical model in *MATLAB/Simulink*. The coolant air temperature, three-phase voltages and currents are exported from the physical model and are processed by EKF estimator as inputs. Compared to the temperatures exported from the physical model of the machine, three parts of temperatures can be estimated quite accurately by the EKF estimator. The online EKF estimator is independent from the machine control algorithm and can work under any speed and load condition if the stator current is nonzero current system.

***Keywords*—**Asynchronous machine, extended Kalman filter, resistance, simulation, temperature estimation, thermal model.

I. Introduction

WIRELESS sensor network has so many important applications such as the monitoring of the environment, the industry and the tracking of things. We focus on the algorithm implementation in one host sensor node and the input signals acquired from distributed sensor nodes. As a sensor node is low-cost, low-power, weak calculation and small in memory size, the algorithm should be simple and efficient so that it can be implemented in a sensor node. The thermal behavior monitoring system of an asynchronous machine is examined for the further implementation on a sensor node.

Asynchronous machines are widely used due to their low cost, robustness and low maintenance requirements. The thermal behavior of an asynchronous machine largely determines the maximum lifetime, the ability of over-load and also the accuracy in high-performance controller [1]. Thermal stress and exceeding of the temperature protection class may be the reason for insulation deterioration as well as rotor faults [2]. So the temperature monitoring of the stator winding, rotor cage and stator core can be used for thermal fault detection and predictive monitoring. It can help the machine to extend the life span and contribute much to the high performance of the machine [2].

The most common method is the construction of a temperature measurement system using mounted sensors. Sensors can be fixed on the surface of the stator core and embedded inside the stator winding. However, it is difficult to acquire signals from the rotor while in operation. Local temperature measurement, hot-spot measurement and bulk measurement are described in [3]. Wireless sensor networks can be used to acquire the rotor temperature, but the high cost and the instability would be an obstacle for the production [4], [5]. Two other types of indirect approaches are the temperature calculation based on the thermal model only, and the method based on the estimation of resistive parameters. Thermal analysis based on lumped-parameter thermal network, finite-element analysis, and computational fluid dynamics are considered [6]. The design of a state-of-the-art rotor temperature monitoring system for contact measurement was proposed [7]. Based on the stator windings resistance variation with temperature, a sensorless internal temperature monitoring method for induction motor is introduced [1]. J.K.AI-Tayie [8] proposed a method to estimate the rotor and stator temperatures using the extended Kalman filter. However, only the temperatures of rotor cage and stator winding can be estimated. Moreover, it must be assumed that there is no rise in the coolant air temperature.

The thermal modeling of the machine is a complex multi-disciplinary problem, and it must also evaluate the main internal losses of the machine [9]. The most frequent estimation techniques rely on a calculation of impedance in steady state [10], [11] or on an extended Kalman filter. The estimation of the stator resistance R_s and rotor resistance R_r have presented in [8] and [12], and none of them can estimate the resistances simultaneously.

Combining the electrical and mechanical model with a simplified thermal model, an online approach to estimate the temperatures of stator windings, rotor cage and stator core is proposed. The extended Kalman filter can process the three-phase voltages, currents and the coolant air temperature. This paper defines the state-space equations of the system and how to implement the temperature monitoring system using the extended Kalman filter step by step to estimate the three temperatures of the machine directly. The state-space of the system is presented in Section II. Section III illustrates the implementation of EKF and the tuning of the covariance matrix. In Section IV, the EKF estimator is performed in *MATLAB/Simulink* and the simulation results are discussed. Finally, the conclusions are given in the last section.

II. The Model of the System

EKF algorithm requires a state-space model of the whole system which consists of the electrical and mechanical models

Yi Huang is with the Department Energy and Automation Technology, Technische Universitaet Berlin, Berlin, 10623 Germany (e-mail: yi.huang@campus.tu-berlin.de).

Clemens Guehmann is with the Department Energy and Automation Technology, Technische Universitaet Berlin, Berlin, 10623 Germany (e-mail: see http://www.mdt.tu-berlin.de/menue/mitarbeiter/leitung/).

of the asynchronous machine in the a reference frame, and also the simplified thermal model of the machine.

A. The Model of the Asynchronous Machines

The twin-axis reference frame is used to build the electrical model of the three-phase asynchronous machine. The voltage equations in arbitrary reference frame are often written in the form below:

$$v_{qs} = R_s i_{qs} + \omega\lambda_{ds} + \lambda'_{qs} \tag{1}$$

$$v_{ds} = R_s i_{ds} - \omega\lambda_{qs} + \lambda'_{ds} \tag{2}$$

$$v_{qr} = R_r i_{qr} + (\omega - \omega_r)\lambda_{dr} + \lambda'_{qr} \tag{3}$$

$$v_{dr} = R_r i_{dr} - (\omega - \omega_r)\lambda_{qr} + \lambda'_{dr} \tag{4}$$

$$\lambda_{qs} = L_s i_{qs} + L_m(i_{qs} + i'_{qr}) \tag{5}$$

$$\lambda_{ds} = L_s i_{ds} + L_m(i_{ds} + i'_{dr}) \tag{6}$$

$$\lambda_{qr} = L_r i_{qr} + L_m(i_{qs} + i'_{qr}) \tag{7}$$

$$\lambda_{dr} = L_r i_{dr} + L_m(i_{ds} + i'_{dr}) \tag{8}$$

where v_{qs}, v_{ds} are d-q stator voltages. v_{qr}, v_{dr} are d-q rotor voltages. i_{qs}, i_{ds} are d-q stator currents. i_{qr}, i_{dr} are d-q rotor currents. R_s, R_r are stator and rotor resistance. ω is the reference frame speed and ω_r is the rotor electric speed. λ_{qs}, λ_{ds}, λ_{qr} and λ_{dr} are stator and rotor flux linkages in d-q axis. L_s, L_r are stator and rotor inductances and L_m is mutual inductance.

In order to reduce the number of variables, stator current i_{ds} and i_{qs}, rotor current i_{dr} and i_{qr} in twin-axis stator reference frame is selected. The value of ω is zero, and $\sigma = L_s L_r - L_m^2$. The final equations can be rearranged into state-space format:

$$\begin{aligned}\sigma i'_{ds} = &-R_s L_r i_{ds} + L_m^2 \omega_r i_{qs} + R_r L_m i_{dr} \\ &+ L_r L_m \omega_r i_{qr} + L_r v_{ds}\end{aligned} \tag{9}$$

$$\begin{aligned}\sigma i'_{qs} = &-R_s L_r i_{qs} - L_m^2 \omega_r i_{ds} + R_r L_m i_{qr} \\ &+ L_r L_m \omega_r i_{qr} + L_r v_{qs}\end{aligned} \tag{10}$$

$$\begin{aligned}\sigma i'_{dr} = &-R_s L_m i_{ds} - L_s L_m \omega_r i_{qs} - R_r L_s i_{dr} \\ &- L_s L_r \omega_r i_{qr} - L_m v_{ds}\end{aligned} \tag{11}$$

$$\begin{aligned}\sigma i'_{qr} = &L_s L_m \omega_r i_{ds} + R_s L_m i_{qs} + L_s L_r \omega_r i_{dr} \\ &- R_r L_s i_{qr} - L_m v_{qs}\end{aligned} \tag{12}$$

The general mechanical model of the system comes from the torque balance equation which can be expressed as:

$$T_e = F_f \omega_r + J\omega'_r + T_l \tag{13}$$

where T_e is the electromagnetic torque and T_l is the load torque. F_f is the friction constant and J is total inertia. The total electromagnetic torque of the asynchronous machine T_e can be expressed by the stator and rotor current component in twin-axis reference frame:

$$T_e = p_n L_m (i_{qs} i_{dr} - i_{ds} i_{qr}) \tag{14}$$

where p_n is the number of pair pole. From (13), (14), the state-space of the rotor speed is shown below:

$$\omega'_r = \frac{p_n L_m}{J}(i_{qs} i_{dr} - i_{ds} i_{qr}) - \frac{F_f \omega_r}{J} - \frac{T_l}{J} \tag{15}$$

B. The Thermal Model of the Asynchronous Machines

The thermal model of the machine is constructed based on the thermal equivalent network established in [13]. The heat of the machine is generated from the power losses, which consists of the losses of stator winding, losses of the stator core, losses of the rotor cage, losses of the rotor core, friction losses and stray load losses [14]. There is no core in the squirrel cage rotor, so the losses of rotor core is taken as zero. In order to simplify the thermal model, the friction losses and the stray load losses are dissipated to the environment and not contribute to the thermal transfer. The simplified thermal model equations in [13] can be written as following equations:

$$T'_{sw} = \frac{-R_{sw} T_{sw}}{C_{sw}} + \frac{R_{sw} T_{sc}}{C_{sw}} + \frac{P_{sw}}{C_{sw}} \tag{16}$$

$$T'_{rc} = \frac{-R_{rc} T_{rc}}{C_{rc}} + \frac{R_{rc} T_{sc}}{C_{rc}} + \frac{P_{rc}}{C_{rc}} \tag{17}$$

$$\begin{aligned}T'_{sc} = &\frac{-R_{sw} T_{sw}}{C_{sc}} + \frac{R_{rc} T_{rc}}{C_{sc}} + \frac{R_{sc} T_c}{C_{sc}} \\ &+ \frac{(R_{sw} + R_{rc} + R_{sc}) T_{sc}}{C_{sc}} + \frac{P_{sc}}{C_{sc}}\end{aligned} \tag{18}$$

where T_{sw}, T_{rc}, T_{sc} and T_c are temperatures above ambient of stator winding, rotor cage, stator core and coolant air respectively. R_{sw}, R_{rc} and R_{sc} are thermal resistances. C_{sw}, C_{rc} and C_{sc} are thermal capacitances. P_{sw}, P_{rc} and P_{sc} are the losses respect to stator winding, rotor cage and stator core.

In the simplified thermal model, P_{sw}, P_{rc} are ohmic losses, and P_{sc} is the frequency-dependent iron losses, R_s, R_r are the DC resistance, in ohms, between any two line terminals, ω_m is the mechanical speed of the rotor in rad/s, k_{iron} is the iron loss constant. The losses can be represented as:

$$P_{sw} = \frac{3}{2} R_s (i_{qs}^2 + i_{ds}^2) \tag{19}$$

$$P_{rc} = \frac{3}{2} R_r (i_{qr}^2 + i_{dr}^2) \tag{20}$$

$$P_{sc} = k_{iron} \omega_m^2 \tag{21}$$

C. The Combined Model of the System

In order to combine the model of the asynchronous machines and the thermal model into a series of integrated state-space equations, the temperature dependent characteristics of the resistance is used. Both R_s and R_r can be replaced by the following equations:

$$R_s = R_{sRef}(1 + \alpha_s T_{sw}) \tag{22}$$

$$R_r = R_{rRef}(1 + \alpha_r T_{rc}) \tag{23}$$

where R_{sRef} and R_{rRef} are the resistances in the reference temperature. α_s and α_r are temperature coefficients of stator winding (copper) and rotor cage (aluminum).

From (9)-(12), (15), (16)-(18), the final state space system can be acquired by substituting P_{sw}, P_{rc}, P_{sc} expressed in (19)-(20) into (16)-(18), and substituting R_s, R_r in (22), (23) into (9)-(12), (16)-(18). Summarizing the previous equations,

the system can be rewritten as a 9th-order nonlinear continuous time-variant system in the state space model form:

$$\mathbf{x}'(t) = \mathbf{A}(\mathbf{x}(t))\mathbf{x}(t) + \mathbf{B}(t)\mathbf{u}(t) \tag{24}$$

$$\mathbf{z}(t) = \mathbf{C}\mathbf{x}(t) + \mathbf{D}(t)\mathbf{u}(t) \tag{25}$$

where:

$$\mathbf{x} = [i_{ds}, i_{qs}, i_{dr}, i_{qr}, \omega_r, T_l, T_{sw}, T_{rc}, T_{sc}]^{\mathrm{T}} \tag{26}$$

$$\mathbf{z} = [i_{ds}, i_{qs}]^{\mathrm{T}} \tag{27}$$

$$\mathbf{u} = [v_{ds}, v_{qs}, T_c]^{\mathrm{T}} \tag{28}$$

$$\mathbf{B}(t) = \begin{bmatrix} \frac{L_r}{\delta} & 0 & 0 \\ 0 & \frac{L_r}{\delta} & 0 \\ \frac{L_m}{\delta} & 0 & 0 \\ 0 & \frac{L_r}{\delta} & 0 \\ 0 & 0 & 0 \\ 0 & 0 & 0 \\ 0 & 0 & 0 \\ 0 & 0 & 0 \\ 0 & 0 & \frac{R_{sc}}{\delta} \end{bmatrix} \tag{29}$$

$$\mathbf{C} = \begin{bmatrix} 1 & 0 & 0 & 0 & 0 & 0 & 0 & 0 & 0 \\ 0 & 1 & 0 & 0 & 0 & 0 & 0 & 0 & 0 \end{bmatrix} \tag{30}$$

$$\delta = L_s L_r - L_m^2 \tag{31}$$

$$a(t) = (R_s(1 + \alpha_s T_{sw}(t))) \tag{32}$$

$$b(t) = (R_r(1 + \alpha_r T_{rc}(t))) \tag{33}$$

In the state equations, $\mathbf{x}(t)$ is the state vector, $\mathbf{u}(t)$ is the control vector, the system matrix $\mathbf{A}(\mathbf{x}(t))$ defined in (48) is variable with time, $\mathbf{B}(t)$ is the input matrix which is constant. In the measurement equations, $\mathbf{C}(t)$ is the output matrix, $\mathbf{D}(t)$ is the feedthrough matrix which is zero here. The load torque $\boldsymbol{T}$ is considered constant parameter due to the slow variation with time.

III. The Implementation of Extended Kalman Filter Algorithm

The extended kalman filter is a nonlinear version of the Kalman filter which linearizes about an estimation of the current mean and covariance. In general, both the process noise and the measurement noise should be taken into account in the nonlinear system model and measurement model.

$$\mathbf{x}_k = f(\mathbf{x}_{k-1}, \mathbf{u}_{k-1}) + \mathbf{w}_{k-1} \tag{34}$$

$$\mathbf{z}_k = h(\mathbf{x}_k) + \mathbf{v}_k \tag{35}$$

It is necessary to assume that the process w_k and the measurement noise v_k are random white Gaussian noise with zero mean and their variance can be described by covariance matrix Q and R respectively. They can be defined as

$$\mathbf{E}[w(i)w^T(j)] = \mathbf{Q}\delta(i,j) \tag{36}$$

$$\mathbf{E}[v(i)v^T(j)] = \mathbf{R}\delta(i,j) \tag{37}$$

$$\mathbf{E}[W(i)v^T(j)] = 0 \tag{38}$$

$\delta(i,j)$ is a Dirac Delta function variation

$$\delta(i,j) = \begin{cases} 1 & i = j \\ 0 & i \neq j \end{cases} \tag{39}$$

where Q is a 9x9 positive semi-defined matrix and R is 2x2 positive semi-defined matrix. Both of them are constant matrix. The state space of the system is nonlinear.

A. Initialization of the State Vector and Covariance Matrix

As the discrete EKF is a recursive algorithm starting from sampling time $t = 0$, the starting values of the state vector is

$$\hat{x}(0) = E[\mathbf{x}(0)] \tag{40}$$

where the symbol $\hat{}$ indicates estimated value of a state vector. And a 9x9 error covariance matrix is a diagonal matrix as below:

$$\mathbf{P}(0) = Var[\mathbf{x}(0)] \tag{41}$$

B. The Prediction Stage of EKF

The prediction stage equations of EKF are shown in (42) and (43). Equation (42) is used for updating the state vector from previous sampling time k-1 to current time k. Equation (43) is state of updating error covariance matrix.

$$\hat{x}_k^- = f(\hat{x}_{k-1}, u_{k-1}, 0) \tag{42}$$

$$\hat{P}_k^- = F_k P_{k-1} F_k^T + Q \tag{43}$$

where F_k is the process Jacobians at step k

$$\mathbf{F}_k = \left.\frac{\partial f}{\partial \mathbf{x}}\right|_{x=\hat{x}_k} \tag{44}$$

1) The Discretization of the Model: The model above is a continuous time system which can not be processed by computer. Euler's approximation is used to discrete the model, so that the sampled data can be used in the EKF algorithm. According to the definition of derivative, (24) can be rewritten as:

$$\frac{x(k) - x(k-1)}{\tau} = \mathbf{A}_d x(k-1) + \mathbf{B}_d u(k-1) \tag{45}$$

By simplifying the equation above, the new equation can be expressed as:

$$x(k) = (1 + \tau\mathbf{A}_d)x(k-1) + \tau\mathbf{B}_d u(k-1) \tag{46}$$

As $\boldsymbol{A}$ and $\boldsymbol{B}$ are the matrix, the discrete model is

$$x(k) = \mathbf{A}_d x(k-1) + \mathbf{B}_d u(k-1) \tag{47}$$

where $\boldsymbol{A}_d = \boldsymbol{E} + \tau\boldsymbol{A}$ and $\boldsymbol{B}_d = \tau\boldsymbol{B}$, $\boldsymbol{E}$ is 9x9 unit matrix, $\mathbf{C}_d$ is equal to $\mathbf{C}$, τ is the sampling time.

$$\mathbf{A}(\mathbf{x}(t)) = \begin{bmatrix} \frac{-a(t)L_r}{\delta} & \frac{L_m^2\omega_r(t)}{\delta} & \frac{b(t)L_m}{\delta} & \frac{L_rL_m\omega_r(t)}{\delta} & 0 & 0 & 0 & 0 & 0 \\ \frac{-L_m^2\omega_r(t)}{\delta} & \frac{-a(t)L_r}{\delta} & \frac{-L_rL_m\omega_r(t)}{\delta} & \frac{b(t)L_m\omega_r(t)}{\delta} & 0 & 0 & 0 & 0 & 0 \\ \frac{a(t)L_m}{\delta} & \frac{-L_sL_m\omega_r(t)}{\delta} & \frac{-b(t)L_s}{\delta} & \frac{-L_sL_r\omega_r(t)}{\delta} & 0 & 0 & 0 & 0 & 0 \\ \frac{L_sL_m\omega_r(t)}{\delta} & \frac{a(t)L_r}{\delta} & \frac{L_sL_r\omega_r(t)}{\delta} & \frac{-b(t)L_s}{\delta} & 0 & 0 & 0 & 0 & 0 \\ \frac{-p_nL_mi_{qr}(t)}{J} & \frac{p_nL_mi_{dr}(t)}{J} & 0 & 0 & \frac{-B}{J} & \frac{-1}{J} & 0 & 0 & 0 \\ 0 & 0 & 0 & 0 & 0 & 0 & 0 & 0 & 0 \\ \frac{3a(t)i_{ds}(t)}{2C_{sw}} & \frac{3b(t)i_{qs}(t)}{2C_{sw}} & 0 & 0 & 0 & 0 & \frac{R_{sw}}{C_{sw}} & 0 & \frac{R_{sw}}{C_{sw}} \\ 0 & 0 & \frac{3b(t)i_{dr}(t)}{2C_{rc}} & \frac{3b(t)i_{qr}(t)}{2C_{rc}} & 0 & 0 & 0 & \frac{-R_{rc}}{C_{rc}} & \frac{R_{rc}}{C_{rc}} \\ 0 & 0 & 0 & 0 & \frac{k_{iron}\omega_r(t)}{4C_{sc}} & 0 & \frac{R_{sw}}{C_{sc}} & \frac{R_{rc}}{C_{sc}} & \frac{R_{sw}+R_{rc}+R_{sc}}{C_sc} \end{bmatrix} \quad (48)$$

2) The Linearization of the Model: The linearization of the non-linear model plays crucial role in the the implementation of EKF. The linearization is based on the assumption, that the state variables in (26) are constant in one step of the computation. The linearized state equation can be rewritten in a new form:

$$\frac{\partial f}{\partial \mathbf{x}} = \frac{\partial \mathbf{A}_d(k)x(k-1) + \mathbf{B}_d(k)u(k-1)}{\partial \mathbf{x}} \quad (49)$$

And the output equation is below:

$$\frac{\partial h}{\partial \mathbf{x}} = \frac{\partial \mathbf{h}(x(k-1))}{\partial \mathbf{x}} \quad (50)$$

The Jacobian matrix $\mathbf{F}_k$ is defined in (55), where the coefficients are below:

$$f_{15} = \frac{L_m^2 i_{qs}(k) + L_rL_m i_{qr}(k)\tau}{\delta}, f_{17} = -\frac{R_s\alpha_s L_r i_{ds}(k)\tau}{\delta}$$
$$f_{18} = \frac{R_r\alpha_r L_m i_{dr}(k)\tau}{\delta}, f_{25} = -\frac{L_m(L_m i_{ds}(k) + L_r i_{dr}(k))\tau}{\delta}$$
$$f_{27} = -\frac{R_s\alpha_s L_r i_{qs}(k)\tau}{\delta}, f_{28} = \frac{R_r\alpha_r L_m i_{qr}(k)\tau}{\delta}$$
$$f_{35} = -\frac{L_m L_s i_{qs}(k) + L_s L_r i_{qr}(k)\tau}{\delta}, f_{37} = \frac{R_s\alpha_s L_m i_{ds}(k)\tau}{\delta}$$
$$f_{38} = -\frac{R_r\alpha_r L_1 i_{dr}(k)\tau}{\delta}, f_{45} = \frac{L_m L_s i_{ds}(k) + L_s L_r i_{dr}(k))\tau}{\delta}$$
$$f_{47} = \frac{R_s\alpha_s L_m i_{qs}(k)\tau}{\delta}, f_{48} = -\frac{R_r\alpha_r L_s i_{qr}(k)\tau}{\delta}$$
$$f_{77} = 1 + \frac{3(R_s\alpha_s(i_{ds}(k)^2 + i_{qs}(k)^2) - R_{sw})\tau}{2C_{sw}}$$
$$f_{88} = 1 + \frac{3(R_r\alpha_r(i_{dr}(k)^2 + i_{qr}(k)^2) - R_{rc})\tau}{2C_{rc}}$$
$$f_{99} = 1 - \frac{(R_{sw} + R_{rc} + R_{sc})\tau}{C_{sc}}$$

C. The Correction Stage of EKF

$$K_k = P_k^- H_k^T (H_k P_k^- H_k^T + R)^{-1} \quad (51)$$
$$\hat{x}_k = \hat{x}_k^- + K_k(z_k - h(\hat{x}_k^-, 0)) \quad (52)$$
$$P_{k+1} = (I - K_k H_k) P_k^- \quad (53)$$

where H_k is the measurement Jacobian at step k

$$\mathbf{H}_k = \left.\frac{\partial h}{\partial \mathbf{x}}\right|_{x=\hat{x}_k} \quad (54)$$

IV. Simulation Models and Experiment Results

A. The Combined Simulation Models

The model of a squirrel cage asynchronous machine with losses couples with the simplified thermal model using *Dymola*. The squirrel cage asynchronous machine with losses is explained in [14]-[16]. The model can simulate the transient electrical and magnetic behavior as well as six parts of the machine losses. By connecting an internal thermal port of the machine to the thermal port of the simplified thermal model, all the losses can be passed to the thermal circuit. With the complete model, the temperatures of stator wingding, rotor cage and the stator core can be calculated. The simplified thermal mode is shown in Fig. 1, and both the simulation model and the experiment are explained in [13].

All parameters of the asynchronous machine were identified at a test bench. The complete model is shown in Fig. 2.

With the help of the *Dymola-Simulink* interface, the complete model in *Dymola* can also run in a *Simulink* environment [17]. Meanwhile EKF algorithm is implemented as a S-Function in *Matlab/Simulink*, and connected with the complete physical model. In the complete model, the three-phase stator currents are the measurements, the three-phase voltages and the coolant air temperature are the control vector. They can be exported from $DymolaBlock$ as the input of the EKF. The estimated temperature from EKF can be compared with the temperature calculated by the thermal model. The online EKF estimator in Simulink is shown in Fig. 3.

B. The Simulation Results by EKF Estimator

The parameters of the asynchronous machine and the parameters of the thermal model are listed in Tables III-V respectively. The implemented EKF algorithm is independent from the control strategy and the running conditions of the machine. The temperatures of stator winding, rotor cage and stator core can be estimated in any operating condition. Full-load test **S1** and intermittent-load test **S6** have performed in Simulink and the sampling time is 500 μs. The initial error covariance matrix, process noise covariance matrix and measurement covariance matrix are obtained by trial and error method:

$$\mathbf{P}(0) = diag\begin{bmatrix} 5 & 5 & 5 & 5 & 5 & 5 & 0 & 0 & 0 \end{bmatrix}$$

$$\mathbf{F}(k) = \begin{bmatrix} 1-\frac{a(k)L_r\tau}{\delta} & \frac{L_m^2\omega_r(k)\tau}{\delta} & \frac{b(k)L_m\tau}{\delta} & \frac{L_rL_m\omega_r(k)\tau}{\delta} & f_{15} & 0 & f_{17} & f_{18} & 0 \\ \frac{-L_m^2\omega_r(k)\tau}{\delta} & 1-\frac{a(k)L_r\tau}{\delta} & \frac{-L_rL_m\omega_r(k)\tau}{\delta} & \frac{b(k)L_m\omega_r(k)\tau}{\delta} & f_{25} & 0 & f_{27} & f_{28} & 0 \\ \frac{a(k)L_m\tau}{\delta} & \frac{-L_sL_m\omega_r(k)\tau}{\delta} & 1-\frac{b(k)L_s\tau}{\delta} & \frac{-L_sL_r\omega_r(k)\tau}{\delta} & f_{35} & 0 & f_{37} & f_{38} & 0 \\ \frac{L_sL_m\omega_r(k)\tau}{\delta} & \frac{a(k)L_r\tau}{\delta} & \frac{L_sL_r\omega_r(k)\tau}{\delta} & 1-\frac{b(k)L_s\tau}{\delta} & f_{45} & 0 & f_{47} & f_{48} & 0 \\ \frac{-p_nL_mi_{qr}(k)\tau}{J} & \frac{p_nL_mi_{dr}(k)\tau}{J} & \frac{p_nL_mi_{qs}(k)\tau}{J} & \frac{-p_nL_mi_{ds}(k)\tau}{J} & 1-\frac{B\tau}{J} & -\frac{\tau}{J} & 0 & 0 & 0 \\ 0 & 0 & 0 & 0 & 0 & 1 & 0 & 0 & 0 \\ \frac{3a(k)i_{ds}(k)\tau}{C_{sw}} & \frac{3b(k)i_{qs}(k)\tau}{C_{sw}} & 0 & 0 & 0 & 0 & f_{77} & 0 & \frac{R_{sw}\tau}{C_{sw}} \\ 0 & 0 & \frac{3b(k)i_{dr}(k)\tau}{C_{rc}} & \frac{3b(k)i_{qr}(k)\tau}{C_{rc}} & 0 & 0 & 0 & f_{88} & \frac{R_{rc}\tau}{C_{rc}} \\ 0 & 0 & 0 & 0 & \frac{k_{iron}\omega_r(k)\tau}{2C_{sc}} & 0 & \frac{R_{sw}\tau}{C_{sc}} & \frac{R_{rc}\tau}{C_{sc}} & f_{99} \end{bmatrix} \quad (55)$$

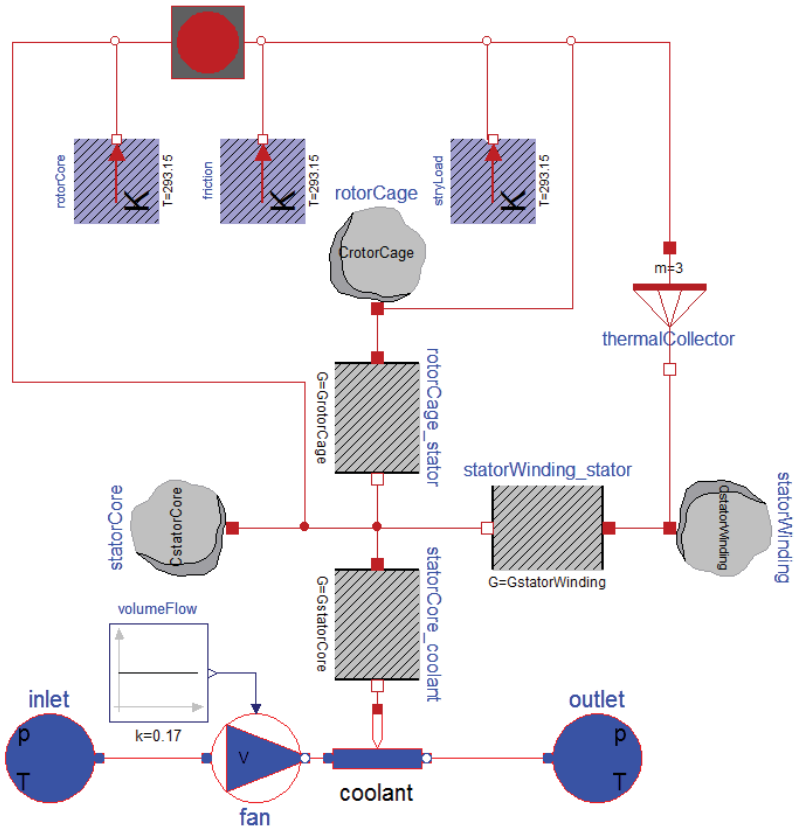

Fig. 1 The Simplified Thermal Model

$\mathbf{Q} = diag\begin{bmatrix} 3 & 3 & 0.5 & 0.5 & 0.01 & 0.1 & 10^{-7} & 10^{-7} & 10^{-8} \end{bmatrix}$ used to evaluate the accuracy of the estimator.

$$\mathbf{R} = \begin{bmatrix} 0.1 & 0 \\ 0 & 0.1 \end{bmatrix}$$

Two experiments are performed. One is the continuous full load **S1** which means the machine runs at the rated condition until the temperatures are stable. Fig. 4 shows the comparison between the temperatures exported from the physical model in *Dymola* and the temperatures estimate by EKF in Simulink. The sampling time is 500 μs and the simulation period is about four hours.

Apart from the deviation for every point, the normalized root-mean-square error (NRMSR) e_{NRMS} defined in (56) is

$$e_{NRMS} = \sqrt{\frac{1}{N}\sum_{i=0}^{N}\left(\frac{y_{mea}(i) - y_{est}(i)}{max(y_{mea}) - min(y_{mea})}\right)^2} \quad (56)$$

The estimated temperatures follow the simulated reference temperatures quite well. The maximum error and the NRMSE value for each region under S1 condition are summarized in Table I.

Another experiment is called **S6** which is an intermittent load with six minutes no-load followed by four minutes full-load. The sampling time is also 500 μs. The results of the temperatures match the simulated reference temperatures very well. Fig. 5 shows the comparison between the temperature simulated and the temperature estimate by EKF under an

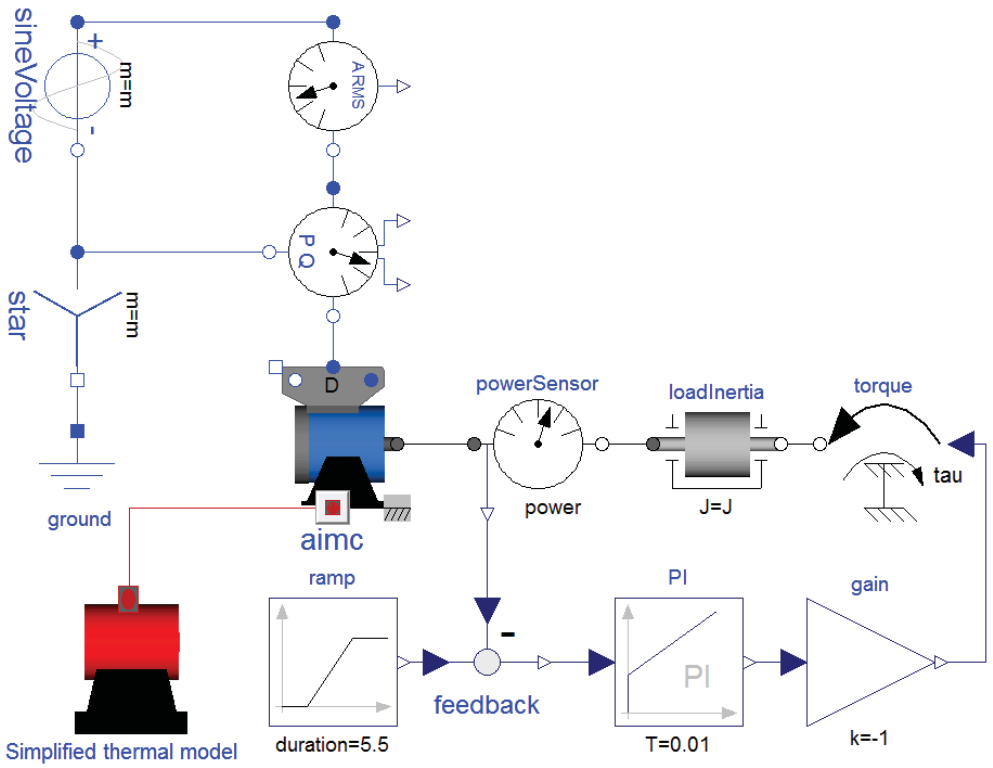

Fig. 2 The Complete Model

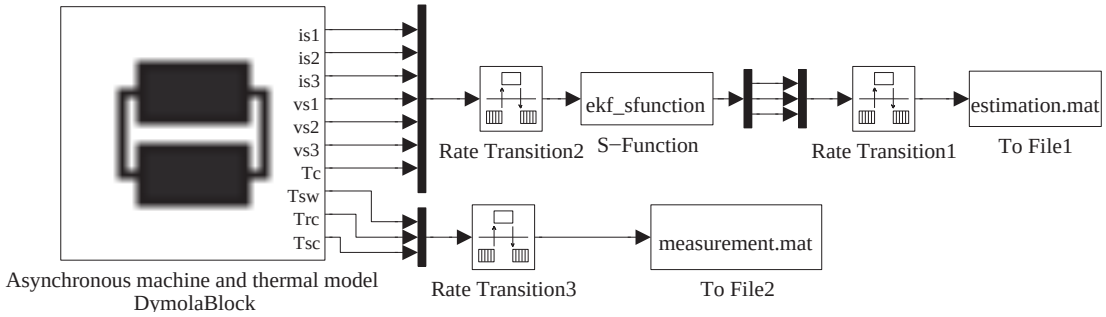

Fig. 3 EKF Estimator in Simulink

TABLE I
THE ERROR AND NRMSE OF THE ESTIMATED TEMPERATURES UNDER S1

Parameters	Maximum Error	NRMSE
Stator winding	1.6°C	2.11%
Rotor cage	3.1°C	2.91%
Stator core	1.2°C	2.05%

intermittent load **S6**. The maximum error and the NRMSE value for each region under S6 condition are summarized in Table II.

TABLE II
THE ERROR AND NRMSE OF THE ESTIMATED TEMPERATURES UNDER S6

Parameters	Maximum Error	NRMSE
Stator winding	1.6°C	1.88%
Rotor cage	2.1°C	3.01%
Stator core	1.8°C	1.86%

V. CONCLUSION

This paper proposed an on-line method to estimate the temperatures of stator wingding, rotor cage and stator core of an asynchronous machine using an extended Kalman filter. By combining the model of the asynchronous machine in twin-axis stator reference frame and the simplified thermal model, the state-space equations have been defined and implemented as a 9th-order extended Kalman filter. The complete temperature simulation model based on [13] is modeled in *Dymola* and runs well compared to the results in [13]. The coolant air temperature, three-phase currents and voltages are exported from the asynchronous machine model in *Dymola* which are the inputs of EKF. Both the *Dymola* model and EKF algorithm complied in an S-Function can be simulated in *MATLAB/SIMULINK*. The estimated temperatures follow the simulated reference temperatures very

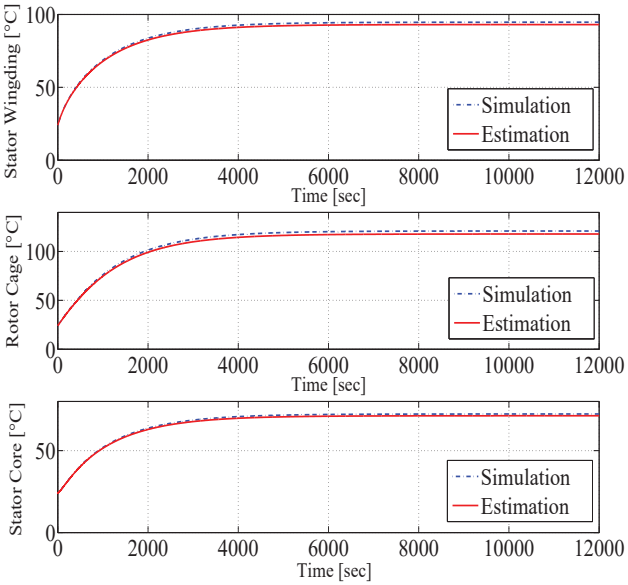

Fig. 4 Comparison of simulated and estimated temperatures under continuous duty S1

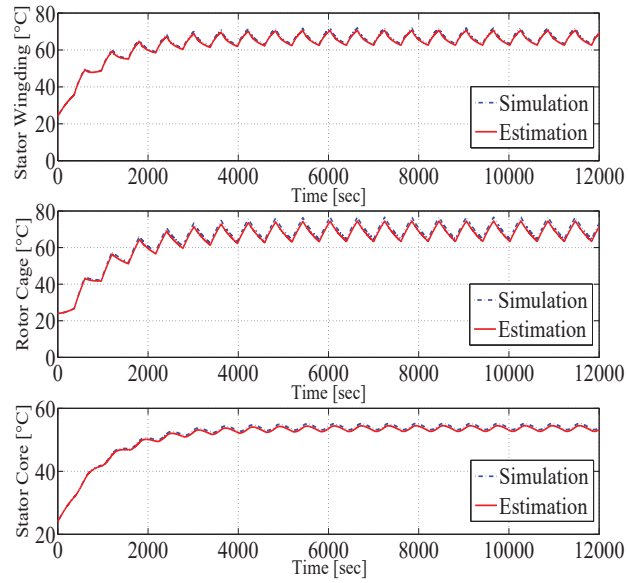

Fig. 5 Comparison of simulated and estimated temperatures under intermittent duty S6

well under both S1 and S6 conditions. The advantages of the algorithm are as follows:

- The estimated temperatures can be obtained by acquiring the three phase stator voltage, current and the coolant air temperature. The rotor speed and the torque can also be estimated simultaneously.
- The estimator is independent from the operation conditions. That means no matter what the rotor speed is, and what the mechanical load is, as long as there are currents through the stator winding, the temperature can be estimated correctly.

APPENDIX

TABLE III
PARAMETERS OF ASYNCHRONOUS MACHINE

Parameters	Symbols	Values
Nominal output	P_m	3 kW
Nominal voltage	V	380 V
Nominal frequency	f	50 Hz
Nominal torque	T	20 N·m
Connection		delta
Pole pair	p_n	2
Stator resistance	R_s	1.9693 Ω
Rotor resistance	R_r	1.8081 Ω
Main reactance	X_m	52.025 Ω
Stator leakage reactance	X_s	2.02 Ω
Rotor leakage reactance	X_r	2.02 Ω
Rotor's moment of inertia	J_r	0.01654 kg.m^2
Iron loss constant	k_{iron}	0.00664 W/(rad/s)^2

TABLE IV
THERMAL CAPACITANCES OF SIMPLIFIED MODEL

Parameters	Symbols	Values
Stator winding capacitance	C_{sw}	3000 J/K
Rotor cage capacitance	C_{rc}	1366 J/K
Stator core capacitance	C_{sc}	7000 J/K

TABLE V
THERMAL RESISTANCES OF SIMPLIFIED MODEL

Parameters	Symbols	Values
Stator winding resistance	R_{sw}	13.8 K/W
Rotor cage resistance	R_{rc}	3.52 K/W
Stator core resistance	R_{sc}	15.3 K/W

REFERENCES

[1] M. O. Sonnaillon, G. Bisheimer, C. D. Angelo, and G. O. Garca, "Online sensorless induction motor temperature monitoring," *IEEE Transactions on Energy Conversion*, vol. 25, no. 2, pp. 273–280, June 2010.

[2] R. Beguenane and M. E. H. Benbouzid, "Induction motors thermal monitoring by means of rotor resistance identification," *IEEE Transactions on Energy Conversion*, vol. 14, no. 3, pp. 566–570, Sep 1999.

[3] P. Tavner, *Condition monitoring of rotating electrical machines*. IET, 2008, vol. 56.

[4] S. Ben Brahim, R. Bouallegue, J. David, T. H. Vuong, and M. David, "A wireless on-line temperature monitoring system for rotating electrical machine," *Wireless Personal Communications*, pp. 1–21, 2016. (Online). Available: http://dx.doi.org/10.1007/s11277-016-3808-5

[5] S. B. Brahim, R. Bouallegue, J. David, and T. H. Vuong, "Modelling and characterization of rotor temperature monitoring system," in *2016 International Wireless Communications and Mobile Computing Conference (IWCMC)*, Sept 2016, pp. 735–740.

[6] G. Welch and G. Bishop, "An introduction to the kalman filter," Chapel Hill, NC, USA, Tech. Rep., 1995.

[7] M. Ganchev, B. Kubicek, and H. Kappeler, "Rotor temperature monitoring system," in *Electrical Machines (ICEM), 2010 XIX International Conference on*, Sept 2010, pp. 1–5.

[8] O. E. E, G. Metin, and B. Seta, "Simultaneous rotor and stator resistance estimation of squirrel cage induction machine with a single extended kalman filter," *Turk. J. Elec. Eng. & Comp. Sic.*, 2010.

[9] Y. Du, T. G. Habetler, and R. G. Harley, "Methods for thermal protection of medium voltage induction motors - a review," in *2008 International Conference on Condition Monitoring and Diagnosis*, April 2008, pp. 229–233.

[10] Z. Gao, T. G. Habetler, and R. G. Harley, "An online adaptive stator winding temperature estimator based on a hybrid thermal model for induction machines," in *IEEE International Conference on Electric Machines and Drives, 2005.*, May 2005, pp. 754–761.

[11] Z. Gao, T. G. Habetler, R. G. Harley, and R. S. Colby, "A novel online rotor temperature estimator for induction machines based on a cascading motor parameter estimation scheme," in *Diagnostics for Electric Machines, Power Electronics and Drives, 2005. SDEMPED 2005. 5th IEEE International Symposium on*, Sept 2005, pp. 1–6.
[12] C. Kral, T. G. Habetler, R. G. Harley, F. Pirker, G. Pascoli, H. Oberguggenberger, and C. J. M. Fenz, "Rotor temperature estimation of squirrel-cage induction motors by means of a combined scheme of parameter estimation and a thermal equivalent model," *IEEE Transactions on Industry Applications*, vol. 40, no. 4, pp. 1049–1057, July 2004.
[13] A. Haumer, C. Kral, V. Vukovic, A. David, C. Hettfleisch, and A. Huzsvar, "A parametrization scheme for high performance thermal models of electric machines using modelica," 2012.
[14] D. Zeng, *Advances in Computer Science and Engineering*. Springer Publishing Company, Incorporated, 2012.
[15] A. Haumer, C. Kral, H. Kapeller, T. Buml, and J. V. Gragger, "The advancedmachines library: Loss models for electric machines," in *Proceedings of the 7th Modelica Conference*, 2009, pp. 847–854.
[16] A. H. C. Kral, "Modelica libraries for dc machines, three phase and polyphase machines," *4th International Modelica Conference*, pp. 549–558, March 2005.
[17] G. Fish, "Dymola-simulink interface," 2011. (Online). Available: http://www.claytex.com/blog/dymola-simulink-interface/

Yi Huang received the B.Eng. degree in vehicle engineering from China Agricultural University, Beijing, China, in 2009, and received the M.Sc. degree in vehicle engineering from China Agricultural University, Beijing, China, in 2011, and is currently pursuing the Dr-Ing. degree at the Technical University of Berlin, Berlin, Germany. His research is about the measurement and diagnosis of an electrical machine on wireless sensor networks.

Clemens Guehmann received the Diplom. degree in electronic technology from the Technical University of Berlin, Berlin, Germany, in 1989, and received the Dr-Ing. degree in Pattern Recognition and Technical Diagnostics from the Technical University of Berlin, Berlin, Germany, in 1995.

He work in Whirlpool company as a development engineer from 1994 to 1995. From 1996 to 2003, he worked in IAV company as a development engineer. Since 2003 he became the professor in the chair of Electronic Measurement and Diagnostic Technology, in the Department of Energy and Automation Technology, Technical University of Berlin. His main research includes Modern Data Processing Methods (e.g. Wavelets) for Automotive Systems, Simulation-, Test- and Calibration Methods for Automotive Electronic Control Units(HiL, MiL, SiL-Simulation), Modeling and Real Time Simulation of Automotive Systems, Pattern Recognition and Technical Diagnosis, Hybrid Vehicle Control Strategies.